ELSEVIER

Geomorphology 42 (2002) 293–310

GEOMORPHOLOGY

www.elsevier.com/locate/geomorph

Morphodynamics of a pseudomeandering gravel bar reach

J. Bartholdy [a,*], P. Billi [b,1]

[a] *Institute of Geography, University of Copenhagen, Øster Voldgade 10, DK 1350 Copenhagen K, Denmark*
[b] *Department of Earth Sciences, University of Ferrara, Corso Ercole I d'Este, n.32, 44100 Ferrara, Italy*

Received 27 June 1999; received in revised form 22 April 2001; accepted 9 May 2001

Abstract

A large number of rivers in Tuscany have channel planforms, which are neither straight nor what is usually understood as meandering. In the typical case, they consist of an almost straight, slightly incised main channel fringed with large lateral bars and lunate-shaped embayments eroded into the former flood plain. In the past, these rivers have not been recognised as an individual category and have often been considered to be either braided or meandering. It is suggested here that this type of river planform be termed *pseudomeandering*.

A typical pseudomeandering river (the Cecina River) is described and analysed to investigate the main factors responsible for producing this channel pattern. A study reach (100×300 m) was surveyed in detail and related to data on discharge, channel changes after floods and grain-size distribution of bed sediments. During 18 months of topographic monitoring, the inner lateral bar in the study reach expanded and migrated towards the concave outer bank which, concurrently, retreated by as much as 25 m. A sediment balance was constructed to analyse bar growth and bank retreat in relation to sediment supply and channel morphology. The conditions necessary to maintain the pseudomeandering morphology of these rivers by preventing them from developing a meandering planform, are discussed and interpreted as a combination of a few main factors such as the flashy character of floods, sediment supply (influenced by both natural processes and human impact), the morphological effects of discharges with contrasting return intervals and the short duration of flood events. Finally, the channel response to floods with variable sediment transport capacity (represented by bed shear stress) is analysed using a simple model. It is demonstrated that bend migration is associated with moderate floods while major floods are responsible for the development of chute channels, which act to suppress bend growth and maintain the low sinuosity configuration of the river.

Keywords: Pseudomeandering; Formative discharge; Lateral bar; Gravel-bed river; Cecina River; Northern Apennines

1. Introduction

Straight or low-sinuosity gravel-bed rivers are common on active continental margins, where they control a significant part of landscape development, and act as important environmental indicators in the geological record (Ibbeken and Schleyer, 1991). This type of river commonly shows a distinct, alternate bar morphology, often referred to as a bedform pattern scaled with channel width (e.g. Jackson, 1975; Ashley, 1990). Some authors (e.g. Ackers and Charlton, 1970; Keller, 1972; Lewin, 1976) regard these large-scale bedforms as incipient meanders, while Yalin (1992, p. 171) describes them as "the 'ca-

* Corresponding author. Fax: +45-35322501.
E-mail addresses: JB@geogr.ku.dk (J. Bartholdy), PBILLI@dicea.unifi.it (P. Billi).
[1] Fax: +39-55495333.

0169-555X/02/$ - see front matter
PII: S0169-555X(01)00092-7

talysts' which accelerate the formation of meanders". In contrast, alternate lateral bars are commonly observed as an equilibrium form (e.g. Bridge et al., 1986; Laronne and Duncan, 1992). This makes low-sinuosity rivers of special interest since they may represent channels at the threshold of meandering that are unable, for some reason, to develop "true" meander bends.

The development of a straight, meandering or braided channel pattern has been documented to depend mainly on discharge, bed gradient (Leopold and Wolman, 1957; Schumm, 1977; Church, 1996) and bed material size (Parker, 1976), although other factors, such as the amount and type of sediment supply and the flow regime, may be relevant in determining channel pattern. Our understanding of the underlying conditions for planform development can be significantly improved by field investigations on the sedimentological, morphological and hydraulic characteristics of low sinuosity channels and by the detailed description of their response to specific run-off events.

Several rivers in Tuscany have a channel planform that is neither straight nor meandering. In the typical case, they consist of an almost straight macro-channel within which a sinuous base-flow channel curves around large lateral bars that force the water towards the opposite bank to erode large, lunate embayments in the alluvial plain. Chute channels commonly develop at the inner side of the lateral bar and interrupt the channel's tendency to meander. For a short time following chute channel formation, two channels may be active and the river morphology bears a strong resemblance to that of a braided stream, though the bar width is much larger than the baseflow channel.

In the past, rivers with these characteristics were not recognised as an individual category and have been indiscriminately classified simply as braided or meandering. It is suggested here that this type of river planform be termed *pseudomeandering*, as first suggested by Hickin (1972). An overview of sedimentological and geomorphological characteristics of pseudomeandering rivers of Tuscany and the description of their channel dynamics according to a five-stage model is reported in the work by Teruggi and Billi (1997).

The primary objectives of this paper are: (i) to describe the channel pattern of a pseudomeandering river in the northern Apennines; (ii) to analyse the

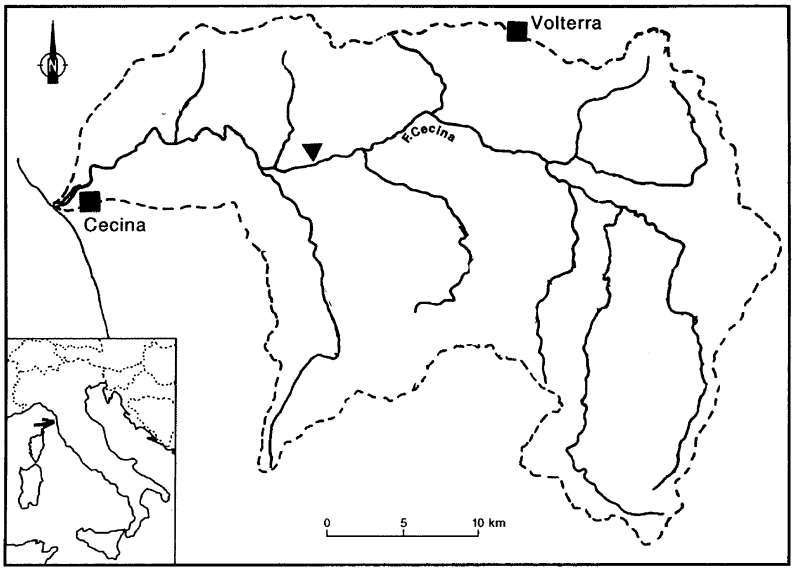

Fig. 1. Location map of the Cecina River valley, situated in the western part of the northern Apennines, southwest of Florence. The study reach is marked with a triangle. The location of the outlet is marked with an arrow on the map of Italy (lower left).

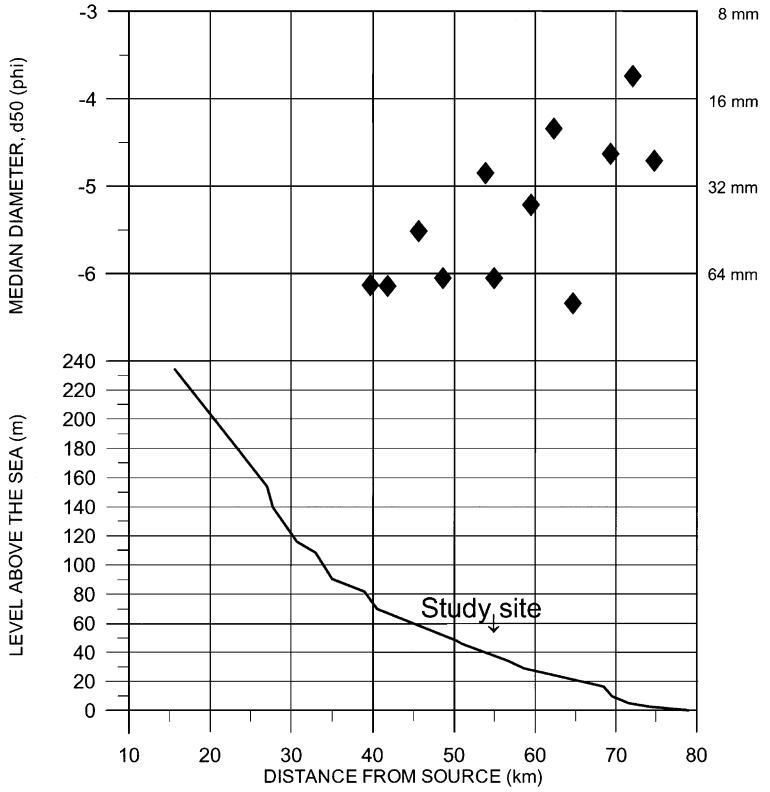

Fig. 2. Below: Longitudinal profile of the Cecina River with the location of the study site. Above: Typical grain-size (D_{50}) of the riffle sediments in the river (from Billi and Paris, 1992).

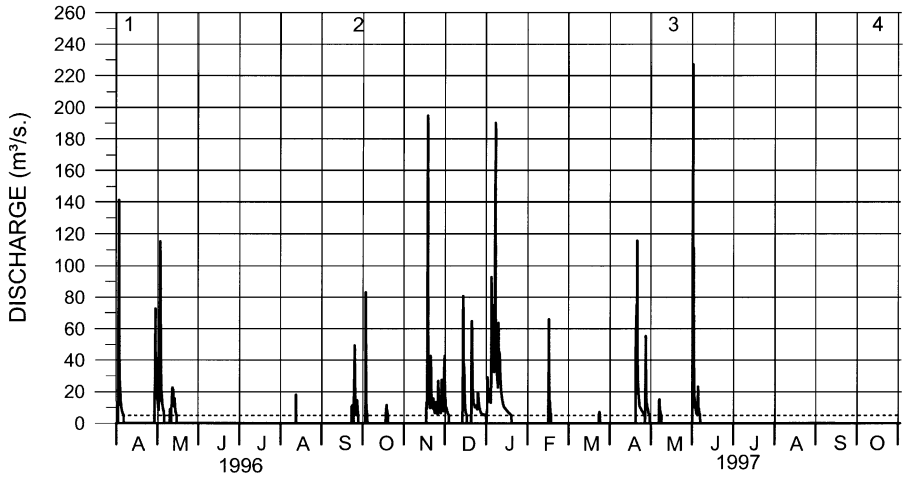

Fig. 3. Discharge records for the study period at Ponte di Monterufoli 2.25 km downstream of the study site. The discharge values are based on a gauging station run by *Servizio Idrografico di Pisa* (Regional Hydrographic Service). Values smaller than 5 m^3/s are not reported. The dates of the four surveys are marked with numbers on top of the diagram.

morphology and texture of a riffle-bar/pool sequence and (iii) to relate the observed morphology and sedimentology to different discharge conditions.

In the study, a reach of the Cecina River was surveyed four times over a period of 18 months, from April 1996 to October 1997.

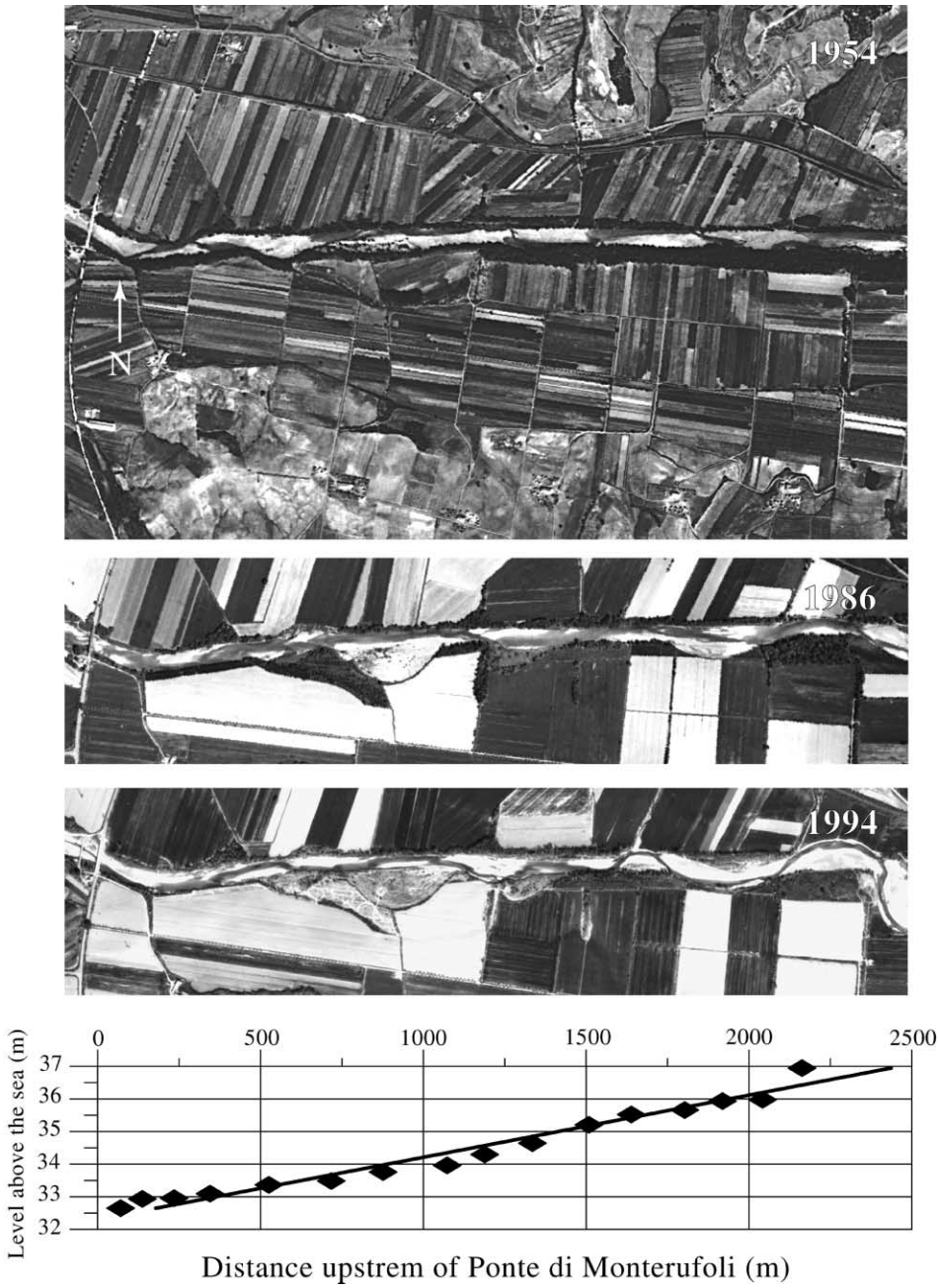

Fig. 4. Vertical aerial photos at the same scale from August 1954; May 1986 and March 1994 of the river reach between the bridge Ponte di Monterufoli (to the left) and the study site, 2250 m upstream of the bridge (last full side bar to the right in the 1986 and 1994 pictures). The scale is indicated by the longitudinal profile underneath. It marks the distance upstream of the bridge. Flow is from right to left.

2. Area of study

The Cecina River is located in central Tuscany, west of Siena. Its catchment area is 900 km^2 and its main stem is about 80-km long (Fig. 1). It is located between the Arno River to the North and the Ombrone River to the South and outflows into the Tyrrhenian Sea at the town of Cecina, approximately 50 km south of Pisa.

The geology of the study area consists mainly of marine sediments which have been subjected to extensive block faulting oriented NW–SE, i.e. perpendicular to the course of the Cecina River (Billi et al., 1991; Carmignani et al., 1995), resulting in a few discontinuities of the otherwise typical concave longitudinal profile of the river (Fig. 2). The study reach, located approximately 55 km from the source and 25 km from the outlet, has an elevation of 37 m a.s.l. and a bed gradient of 1.85×10^{-3}.

Bed material D_{50} (Fig. 2) exhibits a general, though irregular, downstream decrease. Median sizes close to -6 phi (64 mm), 40 km from the source, are replaced by values around -4.5 phi (23 mm), 70 km from the source (10 km from the outlet) (Billi and Paris, 1992).

The average annual precipitation is 900 mm (Cognigni, 1996), but the river is highly ephemeral, with a flashy character, since flood flows are induced mainly by intense cloudbursts, most commonly during autumn and early spring. This is illustrated by the hydrograph covering the study period (Fig. 3). Flow records are obtained from the gauging station at Ponte di Monterufoli, 2250 m downstream of the study site. The maximum discharge during the study

Fig. 5. Vertical aerial photos from August 1954; May 1986 and March 1994 of the study reach marked with a white arrow. Flow is from top to bottom. On the 1994 picture, the surveyed area is marked with a black frame. On the 1986 and 1994 pictures, the black arrow points to a brick-built water well on the property line between two fields. The well fell into the river as a result of bank erosion. In 1994, it was located close to the cut bank. It is now in the process of being buried by the growing side bar (see Fig. 7B).

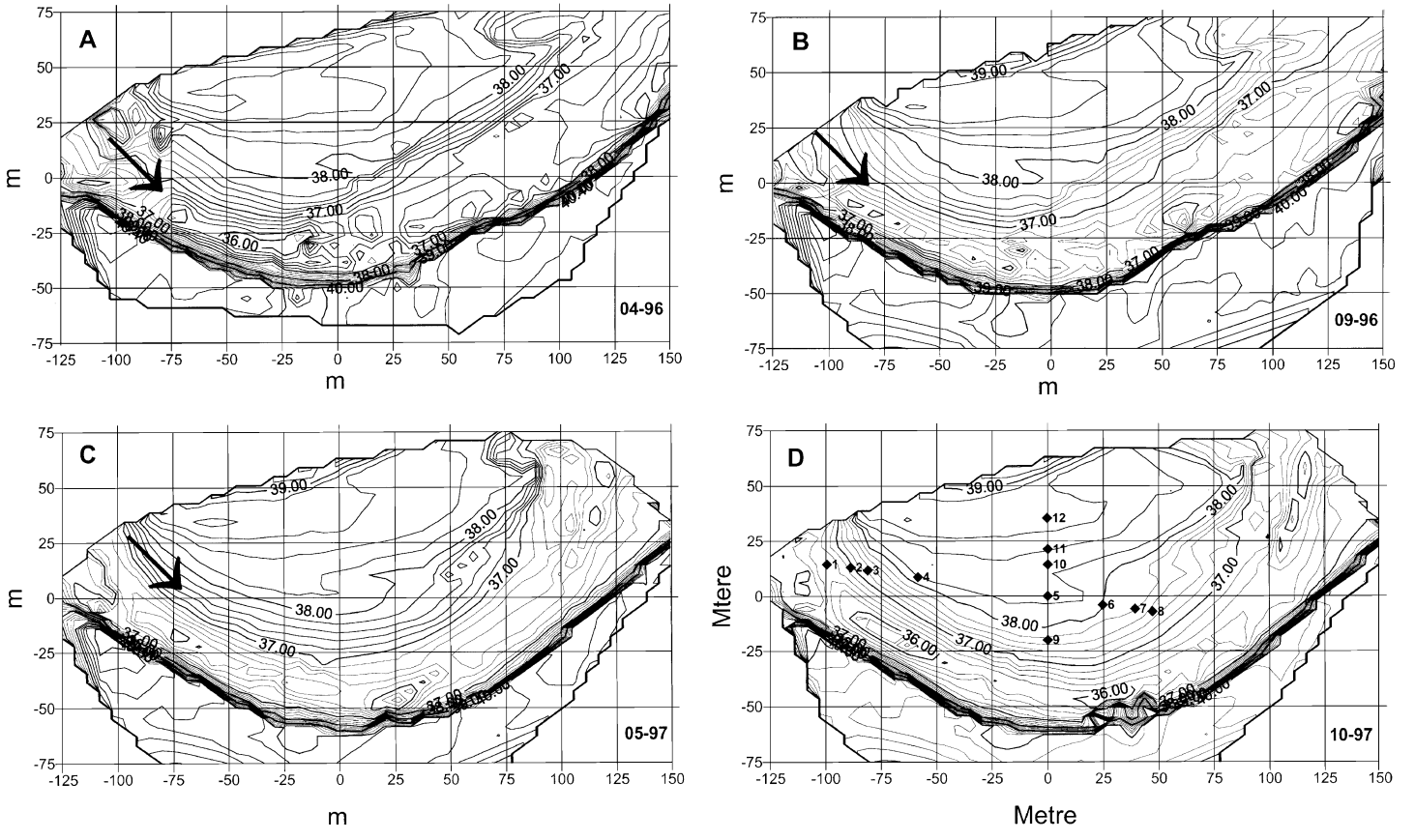

Fig. 6. Maps of the study reach: (A) April 1996, (B) September 1996, (C) May 1997 and (D) October 1997. The flow is from left to right marked with an arrow in (A), (B) and (C), sample locations are indicated in (D). The *X*/*Y*-plane is the same in all four maps referring to 0.0 as the observation point and the *y*-direction as magnetic north. The equidistance of the contour lines (m above sea level) is 0.20 m.

period was 227 m^3/s and discharge exceeded 200 and 100 m^3/s on one and four occasions with a duration of 2 and 42 h, respectively. Discharges usually accepted as descriptive for a river, i.e. $Q_{1.58}$ and $Q_{2.33}$, are 275 and 419 m^3/s, respectively

The general morphology and recent changes in the river valley at the study site are illustrated in Fig. 4. Three vertical aerial photographs at the same scale (August, 1954; May, 1986 and March, 1994) are shown together with a diagram of the riverbed profile derived from levelling between the flow gauge and the study site. The main valley floor is 800–1000-m wide and somewhat less inclined (1.3×10^{-3}) than the riverbed. The elevations of the valley at the flow gauge and the study site are 36.5 and 40 m a.s.l., respectively (Carta Tecnica Regionale 1:5000, 1979).

The change in land use between the dates of the two first areal photographs is striking. In 1954, the valley was tapestried with many small fields, while in 1986 (as well as at present) larger cultivated plots are seen. This change took place in the valley bottom and the surrounding hillsides. By contrast, further inland, farm abandonment during the 1950s and 1960s has left former upland fields uncultivated, causing a general decrease in the sediment supply to the river (Billi and Rinaldi, 1997). During the same period, the sediment supply deficit had been exacerbated by extensive bed material mining that was ultimately forbidden in the whole of Tuscany in 1978 (Billi and Rinaldi, 1997). The resulting reduction in sediment supply resulted in channel incision and the river cut down to form a relatively straight, deep channel with alternate bars. As gravel extraction ceased after 1978, a consistent supply of bed material sediment load was re-established and augmented also by bank erosion associated with channel widening.

In 1954, the reach between the flow gauge and the study site was straight (sinuosity = 1.02), 50-m wide and punctuated by alternating, elongated lateral bars. In 1986, the overall sinuosity was roughly the same (1.03), but, locally, the growth of bars had deflected the baseflow channel against the bank, forming lunate-shaped cut banks, in places cut off by chute channels. In 1994, the sinuosity of the baseflow channel was 1.18. The reach upstream of the study site (the latter is marked with a white arrow on Fig. 5) displays morphological evidence of a complete cycle of change. In 1986, the growth of the prominent bar had forced the left bank to retreat by approximately 100 m with respect to the 1954 picture, and vegetation had covered the innermost, upstream part of the bar, compensating for approximately half of the opposite bank retreat. Between 1954 and 1986, the river widened, the alternate bar configuration moved about 140-m downstream and the sinuosity of the baseflow channel increased. This development continued, and in 1994, an additional erosion of about 120 m was related to a rotating channel migration. It is characteristic that during this massive cutbank retreat, the transition zone between this and the downstream bend was fixed in its original position. This downstream bend was chosen as the study site because here the lateral bar has constantly grown from 1986 to the present, altering the local flow conditions and approaching the threshold condition for a chute cut off, although a cut off has not, as yet, occurred. Bar expansion was associated with almost equivalent bank erosion opposite. The black arrow in the 1986 picture (Fig. 5) marks a water well, which fell into the river some time before 1994, and is now being buried by the growing bar on the opposite bank (Fig. 7B).

3. Methods

The topography of the study site was surveyed using a total station. Within the 300-m-long reach, the survey established 15 detailed cross-sections. Elevations were surveyed by levelling and referred to a level of 33.00 m a.s.l., corresponding to the staff 0-reference of the Regional Hydrographic Service gauging station at *Ponte di Monterufoli*, 2.25 km downstream of the study site.

During the last field campaign (October 1997), 21 bed material samples were collected from the bar, along a longitudinal transect, extending from the upstream riffle to the downstream pool, and along a transverse transect, coinciding with the maximum bar width (Fig. 6D). At each sampling point, surface (one D_{max} thick top layer) and subsurface samples were shovelled into 10-l buckets. In places with sediment finer than 20 mm, a single bulk sample of 0.5 l was collected. The gravel samples were truncated in the

field at 20 and 2 mm. The two sub-samples finer than 20 mm were weighed with an accuracy of ± 5 g and split samples were sent to laboratory for standard sieve and Andreassen pipette analysis at 1/4 phi intervals. The coarse fraction was spread out on a 1 × 1-m black plate with white, 10-cm-long bars for scale. Vertical photos were taken from a tripod and processed by means of WinChips (1998) image analysing software. The area of every particle projection was measured with an accuracy of 1 mm^2, and particle diameter was calculated as the diameter of the circle with the same area as the particle projection. This diameter and a particle density (r_s) of 2650 kg/m^3 were taken to calculate the volume of the equivalent sphere, V_S, and the single particle frequency by weight of the coarse fraction as: $f(\%) = V_S r_S (W/W_S) \times 100$, where W is the weight of the coarse fraction and W_S is the total weight of the related equivalent spheres. The sub-sample results were combined into a total grain-size distribution, based on original fraction frequencies.

4. Sediment

Bed material D_{50} and the topography of the study reach measured in April 1996 and October 1997, are shown in Fig. 8. The sediment on top of the right bank is very fine ($D_{50} = 0.004$ mm) and represents approximately 2 m of overbank deposits resting on coarse-grained bar deposits at the base of the cut bank. When undermined by erosion, this massive, fine-grained layer collapses to form large (as much as 2 m in diameter) mud blocks, which come to rest the base of the cut bank (Fig. 7A).

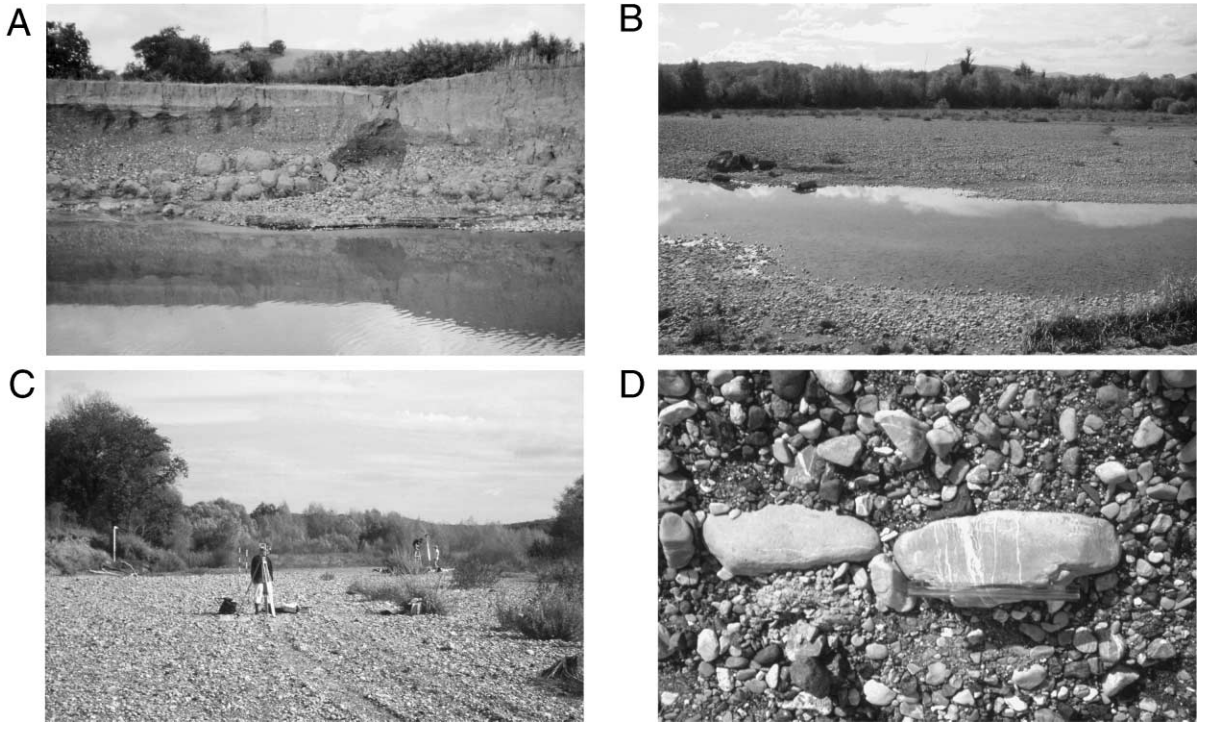

Fig. 7. Photos of the study reach taken in October 1997. (A) The concave cut bank (approximately 4-m high). Notice the old gravel bar at the base overlain by the fine-grained overbank deposits. Parts of the eroded overbank deposits are left in form of giant "mud blocks" at the cliff-foot. (B) The upstream part of the study reach lateral bar viewed from the cut bank. Notice the old water well to the left (see Fig. 5), now in the process of being buried by the prograding bar. (C) The gravel bar during the October 1997 survey. In foreground, the theodolite total station is installed over the observation point. In the distance, the gravel is being sieved and the coarse fraction photographed. (D) A close up of the largest particles on the bar surface near the observation point. Notice the 30-cm-long ruler for scale.

The grain size of bar surface sediment gradually decreases from the low-flow channel margin to the inner part of the bar, reflecting a transition to finer overbank deposits. In the longitudinal profile (Fig. 8), notwithstanding some scatter, a downstream fining is also evident for both surface and subsurface samples. A combination of the subsurface grain size distributions proportional to the deposition on the bar has a mean grain size of − 1.5 phi (2.9 mm) and a sorting coefficient of 2.3 phi. Therefore, though the bar on the surface seems to be dominated by coarse gravel, the bar growth is based on material in the sand-gravel transition.

Visual examination of composite distributions of subsurface samples (Fig. 9) reveals the occurrence of distinctive sub-populations, combined in variable proportions. In the riffle and bar stoss sides, a coarse sub-population with a mean grain size of about − 5.5 phi (45 mm) is abundant and represents the concentration of coarse particles associated with peak flood phases when coarser particles are entrained and transported. In gravel-bed rivers, selective transport has been observed by few authors (e.g. Lenzi et al., 1999) to prevail for discharges ranging from one to two times critical discharge, while conditions favourable to equal mobility are postulated to occur above

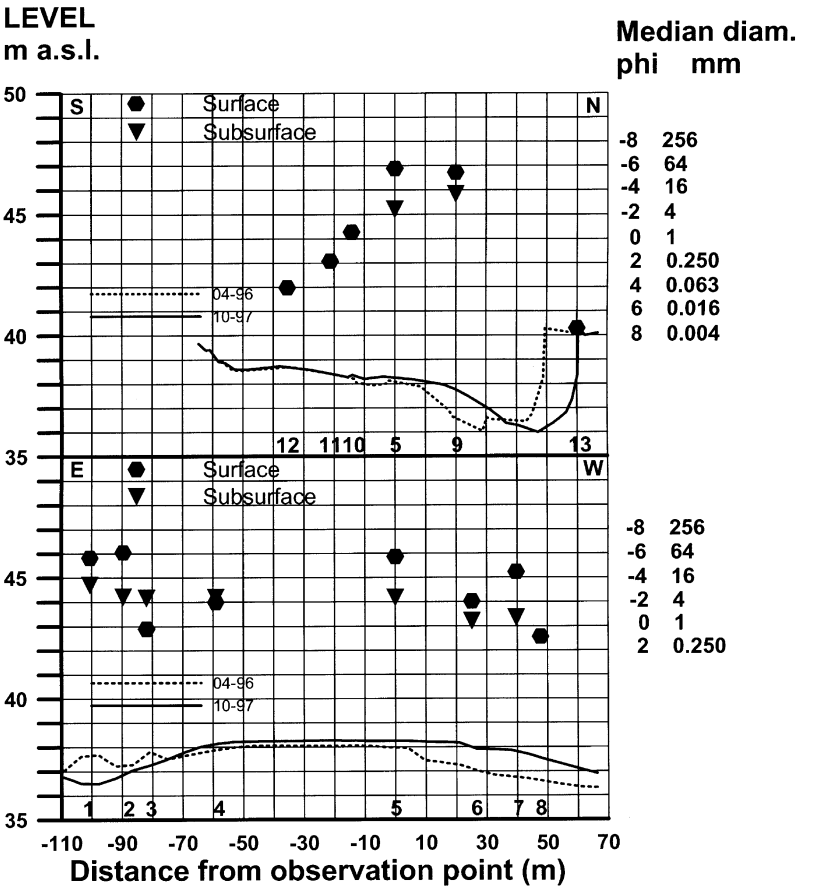

Fig. 8. D_{50} and topographical change in the sampling transects. Above: Cross-section profiles of the study reach. Diamonds and triangles represents surface and subsurface D_{50}, respectively, referred to the October 1997 survey. Flow is away from reader. Below: Longitudinal profile across the bar. Sediment samples symbols as above. Flow is toward the right. In places where a visual, field examination showed no substantial difference between surface and subsurface material, only surface samples were collected. The numbers on the bottom of each diagram refers to the sample numbers shown on the map of Fig. 6D.

this range. The finer mode, on the other hand, represents bedload moving across the bar head that was deposited during the receding flow. The second and third diagrams in Fig. 9 represent material deposited on the bar in the longitudinal and transverse transects respectively (Fig. 8). Three sub-populations are present: a coarse one, as discussed above and two finer washed out from the poorly sorted, fine sediment of the riffle and the stoss side. In the longitudinal transect, deposited material is dominated by the central intermediate population but all three populations are clearly visible. The deposited material, across the bar, is dominated by the fine population, with the other two forming a coarse tail.

5. Bar migration and bank retreat

Contour maps of the study reach (Fig. 6), show the 275-m-long bar, the pool and the cut bank associated with it. During the monitoring period, the bar grew transversely while both its upstream and downstream parts were eroded. As the bar became wider and shorter, the channel decreased its radius of curvature from 170 to 110 m and migrated towards the retreating, concave, cut bank.

Bank erosion was most pronounced (up to 25 m, equivalent to 17 m/year) in the area just downstream of the point of maximum curvature (0 m on the *x*-axis in Fig. 6), whereas, it was zero in the upstream part and less than 5 m in the downstream part of the embayment. Subtracting the October 1997 surface from the April 1996 surface yields the map above the block diagram in Fig. 10. It reveals a total bar deposition of 3.9×10^3 m^3. Most of this deposition occurred in a belt (up to 40 m wide) along the convex, outer side of the bar and represents lateral accretion as the bar migrated towards the cut bank.

Erosion of the upstream and downstream parts of the bar (0.5×10^3 and 1.0×10^3 m^3, respectively)

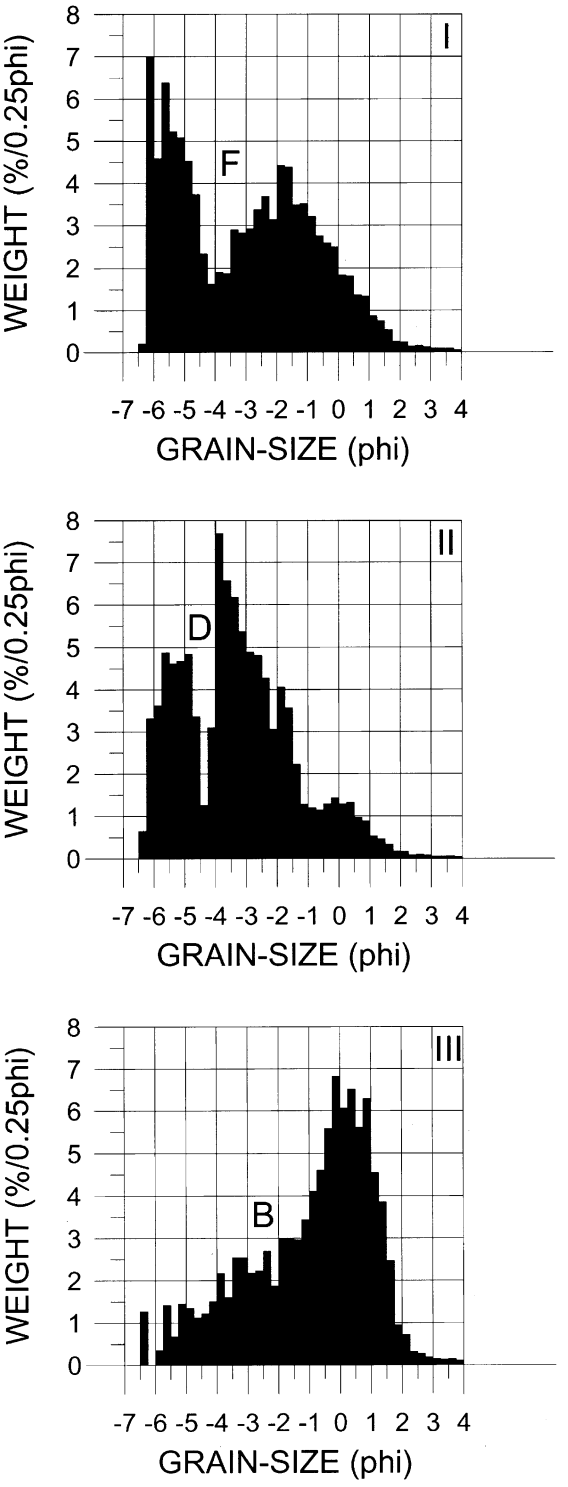

Fig. 9. Representative grain-size distributions of subsurface material in three areas of the study reach: (I) The eroded area at the riffle and stoss side of the bar; (II) The area of deposition in the longitudinal transect; (III) The area of deposition in the cross-section of the bar. The distributions are combined according to the magnitude of erosion/deposition between April 1996 and October 1997 surveys.

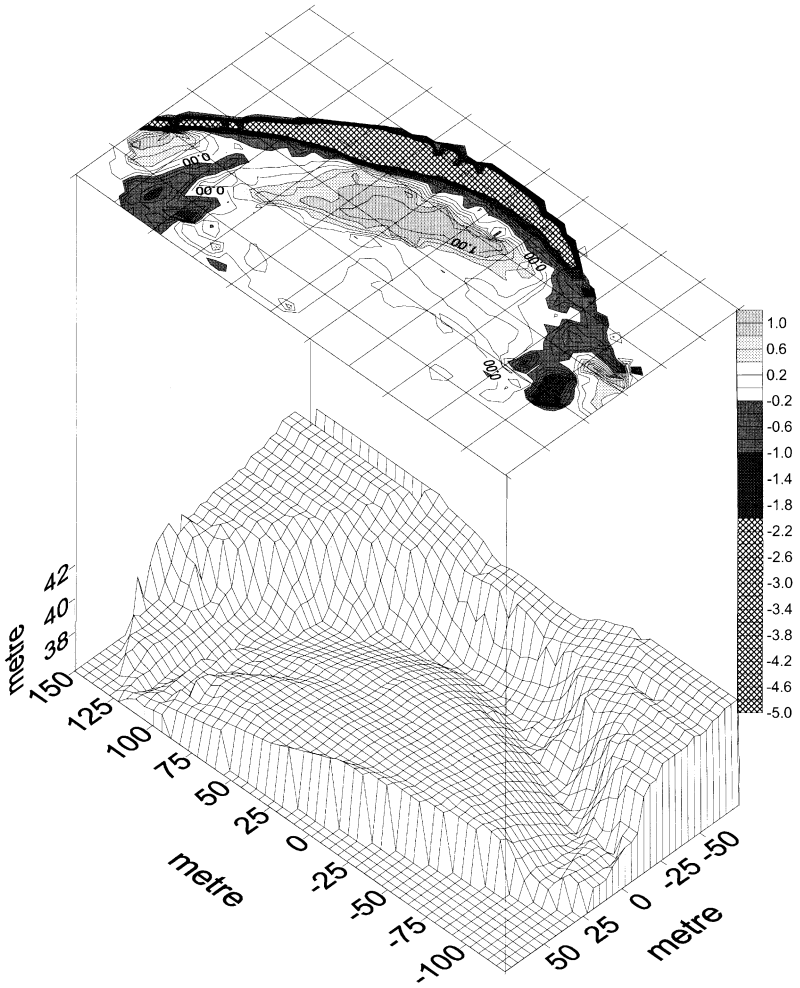

Fig. 10. Block diagram of the study reach based on the October 1997 survey. The flow is from lower right to upper left. In the foreground, the densely vegetated part of the reach is not included in the map. The step up from the base level of the diagram (37-m above the sea) shown here is artificially made by the drawing software. The map above shows the distribution of erosion and deposition between April 1996 and October 1997 surveys. The scale to the right is in metres and shows the legend chosen in order to improve the reading of the 0.2-m equidistance map. Light grey indicates deposition, white is almost no change, dark grey and dashed indicate erosion.

reduced net bar deposition to 2.4×10^3 m^3. Bar deposition and bank erosion are reported as percentages of the totals in Table 1. The temporal variation of deposition followed the discharge pattern (Fig. 3). Bank erosion also reflected the discharge pattern, but was somewhat more sensitive to the duration of floods with moderate to high discharge, as observed in other pseudomeandering rivers of the northern Apennines (Casagli eta l., 1999; Rinaldi and Casagli, 1999), while bar deposition, was apparently more sensitive to the magnitude of higher discharges. Average bank retreat during the 18 months of study was 11 m, equivalent to 7 m/year. The total sediment deficit, that is bank erosion (11.2×10^3 m^3) minus net deposition on the bar, is 8.8×10^3 m^3 or 79% of the bank-eroded material. Hence, inner bar deposition replaced only about 20% of the material eroded from the outer bank, and the incoming supply of sediment was, therefore, significantly smaller than the amount leaving the study reach. The Cecina is an incised river and the present, confined flood plain is about 2 m lower than the old alluvial surface. Releases of relatively large

Table 1
Bar deposition (2.4×10^3 m^3) and bank erosion (11.2×10^3 m^3) expressed as percentages of the total change between the survey periods

	4/1996–9/1996	9/1996–5/1997	5/1997–10/1997
Bar deposition	15	55	30
Bank erosion	14	71	15

amounts of bank material and a sediment deficit were, therefore, to be expected. Even if the sediment pertaining to the old alluvium is omitted, bank erosion is still larger, being more than twice the value of bar deposition. Thus, bar growth is not the cause of bank retreat but is more likely the result of a vain attempt to fill up the space left by the rapidly retreating bank. This constraint to the vertical growth of the bar, paired with wide variations of discharge, seems to prevent the embryonic bends from developing into recognizable meanders and emphasizes the relevance of sediment supply to channel morphology in pseudomeandering rivers.

Erosion in the downstream part of the cut bank (Fig. 10; $x = 120–150$ m) occurred during the first three surveys, along with tightening of the bend radius and with the channel moving away from the cut bank. Erosion definitely ceased between the third and the fourth survey and a secondary sediment accumulation formed between the low-flow channel and the concave bank in the downstream part of the bend (Fig. 10; quadrant $x = 125–150$ and $y = 25–50$). This type of side bar probably results from flow expansion beyond the zone of streambed narrowing, imposed by the downstream hook of the cut bank, and it has been observed in several, similar reaches in the area. Commonly, these bars are composed of coarse sediment and they may play an important role in protecting the downstream part of the cut bank from erosion. This likely accounts for the lack of, or the very slow, downstream progression of bends as observed in other pseudomeandering rivers of the northern Apennines (Brocchi, 1987).

In the central part of the study reach, where bar sedimentation was largest, bank retreat was paralleled by lateral bar growth. This is illustrated in the cross-section shown in Fig. 11. The hydraulic geometry parameters of this cross-section are calculated for vertical increments of 0.10 m for each of the four surveys (Fig. 12).

Cross-sectional area (Fig. 12A) constantly increases from 0 at 36 m a.s.l. to a maximum of about 230 m^2 at 39.8 m a.s.l. (i.e. the elevation of the old alluvial plain margin), while wetted perimeter (Fig. 12B) and width (Fig. 12C) rise in a stepped pattern. The minimum width/depth ratio occurs at an elevation of about 37.8 m a.s.l. This corresponds to a discharge of 100 m^3/s, which is usually exceeded several times a year (Fig. 3). The maximum width/depth ratio (120) (Fig. 12D) occurs at the elevation of the upper part of the bar (38.7 m a.s.l.). Field

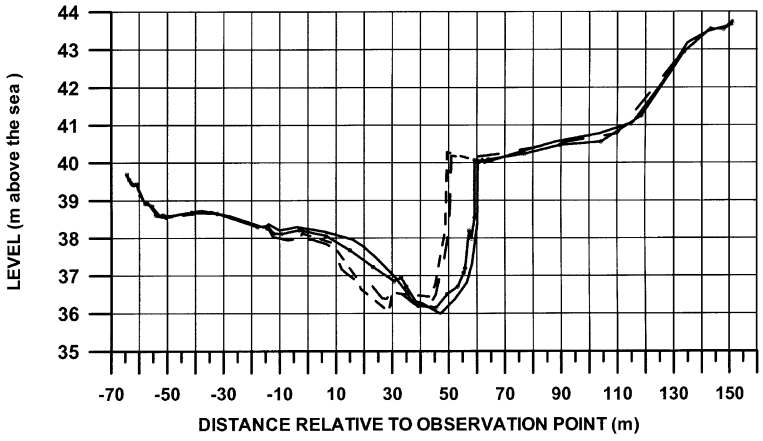

Fig. 11. Cross profile of the study reach in the central part of the bend ($x = 0$; Fig. 6) from each of the four surveys: April 1996, September 1996, May 1997 and October 1997. The succession of the surveys appears from the erosion in the cut bank.

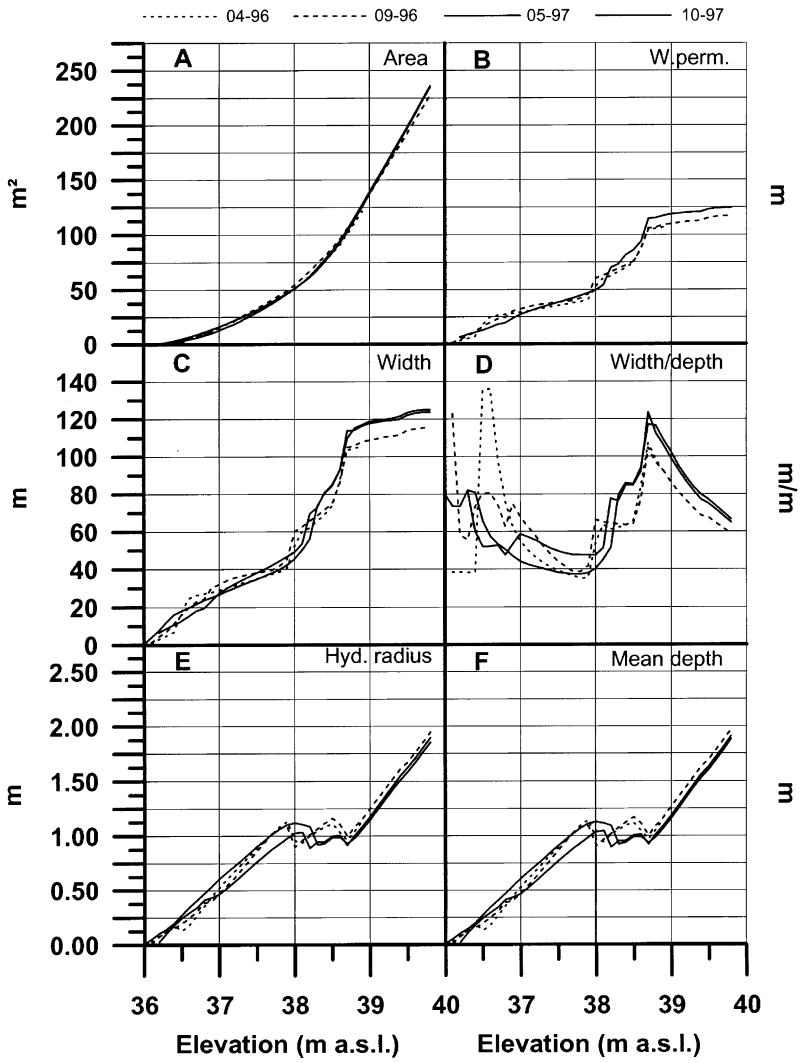

Fig. 12. Morphometric parameters as a function of water level from the four surveys of the reference cross-section at the point of maximum curvature ($x=0$; Fig. 6). (A) Cross-sectional area. (B) Wetted perimeter. (C) Channel width. (D) Width/depth-ratio. (E) Hydraulic radius. (F) Mean depth.

evidence and hydraulic calculations (see Section 6) indicate that this elevation corresponds to a discharge close to $Q_{1.5}$, which is usually regarded as the dominant or bankfull discharge. This finding contrasts the concept of Williams (1978) who identified bankfull conditions as associated with a minimum in the width/depth ratio. Such a difference can be accounted for by the strong asymmetry of the cross-section, with width increasing at a faster rate than mean depth. Between the first and the last survey, the maximum width of the study reach increased by 10%, from 106 to 117 m, and the mean radius of curvature of the baseflow channel decreased from 170 to 110 m. This evolution is most likely a consequence of moderate floods tending to form regular meanders. Field observations (Teruggi and Billi, 1997) indicate the tendency to form regular meanders is interrupted by larger floods. During these floods (Q_{10}–Q_{20}), the bar top is inundated but, given the small size and the confinement of the present flood plain, no over bank

expansion takes place since the flow is constrained within the old alluvial plain banks. The morphological effectiveness of larger floods is therefore fully preserved and they are capable of generating chute cutoffs. Since such chute cutoffs represent the typical final stage in the cycle of adjustment of a pseudomeandering reach (Teruggi and Billi, 1997), two distinct levels of morphologically effective floods and an unbalanced sediment flux seem to be important conditions favouring the development of a pseudomeandering channel pattern.

6. Dynamics

In order to investigate the morphological responses to floods of different magnitude, a simple model has been set up for the study reach. The model does not include the forces arising from change in momentum downstream and across the stream (Smith and McLean, 1984). However, as stated by Dietrich (1987, p. 200) simple calculations omitting these terms "can be used to explain the basic vertically averaged flow pattern in bends". This applies particularly well to long reaches of nearly constant radius of curvature like the one represented by the central cross-section across the study reach.

At the centre of the bar, surface D_{84} (usually selected to match hydraulic roughness, k) is 80 mm (sample 9, Fig. 7), while the mean grain size of deposited material across the bar is 40 mm. If these two grain sizes, regarded as maximum and minimum surface roughness in the profile, are used to calculate Manning's n using $n = k^{1/6}/25.4$, (Engelund and Petersen, 1974), an intermediate n of 0.024 is obtained for the reference cross-section. This value is used in the Manning formula

$$V = n^{-1} d^{2/3} S^{1/2} \quad (1)$$

where V = mean flow velocity, d = mean depth and S = slope, to produce flow and channel dynamic simulations (Fig. 13) by a simple model describing the flow in the bend.

The longstream water slope is altered over the bend as $S = S_c(r_c/r)$ (Allen, 1985), r_c being the radius of curvature at the centreline, r the local radius of curvature and S_c the centreline slope. The local depth is varied over the bend by subtracting the bed topography from the local water level. The water level is calculated across the channel starting from the centreline by adding a local water level change on the base of the transverse slope induced by the local centrifugal acceleration, $S_{tr} = V^2/gr$, where g is the acceleration due to gravity. For a given discharge, the water level over the bend was found by iteration, calculating the local water level and discharge for every metre over the cross-section. The calculations were continued with an increment of 0.01 m of the water level at the centreline, until the sum of the local discharges corresponded to the discharge chosen for the simulation. Bed shear stress was then calculated from $\tau_o = dSg\rho$, where ρ is the density of water.

In the first simulation (Fig. 13A), the largest discharge occurred during the observation period (227 m^3/s on 2/6/1997, close to $Q_{1.5} = 275$ m^3/s) is simulated, based on the October 1997 river morphology. The modelled water level reaches an elevation slightly lower than that associated with the width/depth ratio peak (Fig. 12D). During the flood, at the location where sample 9 was collected, the bar was accreting and bed shear stress reached 16 N/m^2. The corresponding largest moveable particle (D_{max}), calculated using the method of Komar (1989) as discussed in Komar (1996):

$$D_{max} = \left[\tau_0 (0.045(\rho_s - \rho) g D_{50}^{0.6})^{-1}\right]^{2.5} \quad (2)$$

where ρ_s is particle density (2650 kg/m^3), has a size of 60 mm. The coarsest particles in sample 9 are 120 and 70 mm for surface and subsurface, respectively; thus, Komar's equation gives a good prediction, though it underestimates the maximum moveable grain size at the surface. Other equations provide the following values, intermediate between surface and subsurface D_{max}: Baker and Ritter (1975), 84 mm; Williams (1983), 94 mm. A simple critical Shields parameter of $\theta_c = 0.045$ gives 22 mm, which is between surface and subsurface D_{50}, but closer to the latter. Thus, the calculated maximum and median particle sizes of subsurface material are of the right order of magnitude, which supports the applicability of the model.

The other three simulations indicate how a discharge with a recurrence interval of 20 years (818

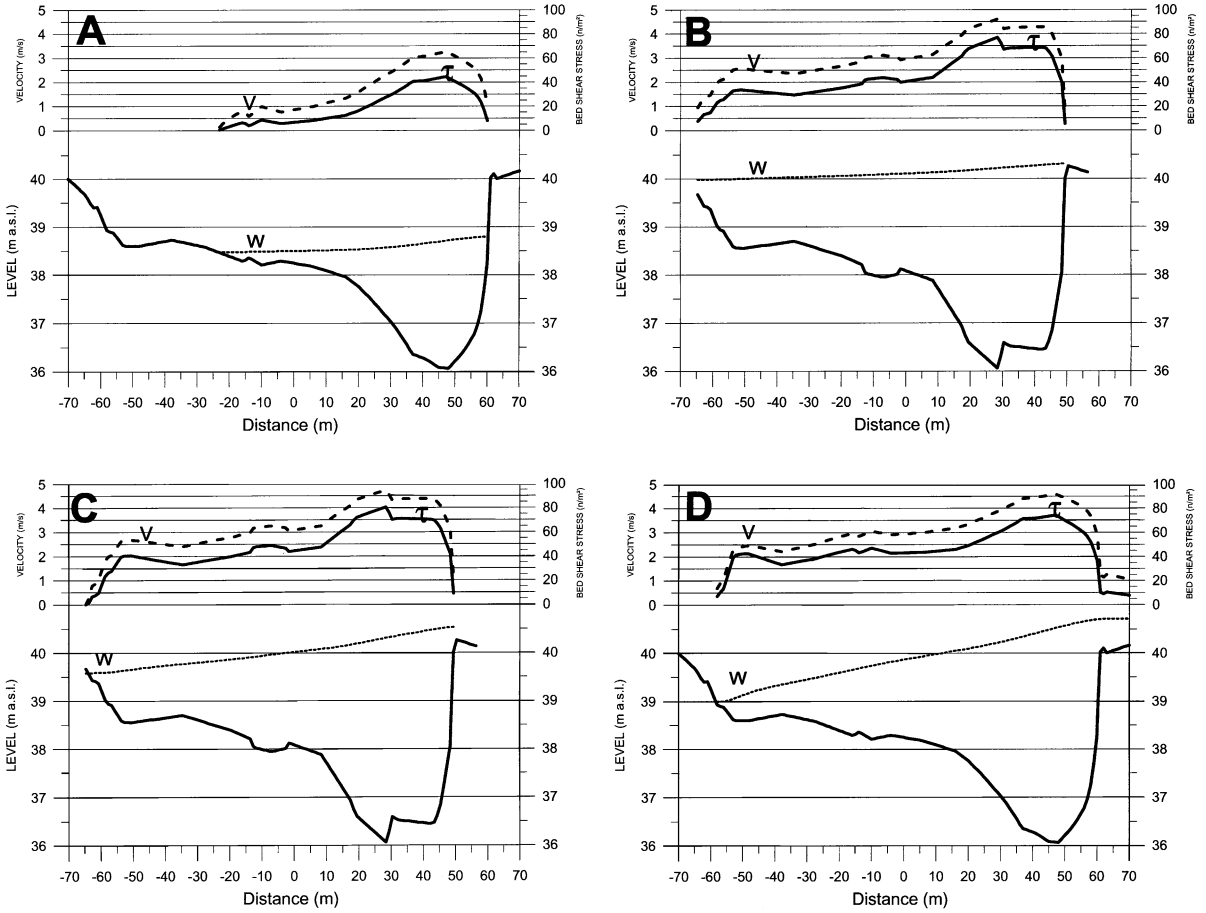

Fig. 13. Simulation of water level, velocity and bed shear stress in the cross profile of the central part of the study reach in four different situations: (A) The highest measured discharge in the study period (June 1997) with topography and radius of curvature of October 1997 survey. (B) Discharge corresponding to a recurrence interval of 20 years with topography from the April 1996 survey and a radius of curvature of 400 m. (C) Discharge corresponding to a recurrence interval of 20 years with topography from the April 1996 survey and a radius of curvature of 170 m. (D) Discharge corresponding to a recurrence interval of 20 years with topography and radius of curvature (110 m) from the October 1997 survey.

m^3/s) would affect the bend in three different morphological situations: (i) the 1986 situation with a radius of curvature of 400 m (estimated from the 1986 aerial photo of Fig. 4) (Fig. 13B). This is a rough approximation, but the only one possible; (ii) the topography and radius of curvature (170 m) from the April 1996 survey (Fig. 13C); (iii) the topography and radius of curvature (110 m) from the October 1997 survey (Fig. 13D).

The patterns of Fig. 13B,C and D are, therefore, controlled primarily by the radius of curvature, which decreased from 400 to 170 and then to 110 m. In simulation b, the water level is just beneath the old floodplain level, while in simulations c and d, the more tightly curved bend forces the inclined water surface over the outer bank and flow depth becomes smaller in the inner part of the bend. Here, bed shear stress increases considerably as a result of the larger longstream slope in the even more tightly curved bend, while elsewhere on the cross profile, shear stress varies according to variations in water depth. The occurrence of a secondary shear stress maximum in the inner part of the bar, around $x = -50$ m, is relevant to channel pattern change. During the three

simulations, this secondary shear stress maximum increases from 34, to 41 and finally to 43 N/m^2. In simulation d, the transition between lower and upper flow regime is reached. In simulations c and d, shear stress in the inner part of the bend exceeds the maximum bed shear stress in the centre of the channel during a 1.5-year flood (simulation a). The simulations show the present bend is so tightly curved that, during a 20-year flood, the flow over the bar produces a bed shear stress, which is large enough to erode a new main channel in the initial form of a chute cut off. Lewis and Lewin (1983) observed that chute cutoff frequency is maximum when the r_c/w ratio (radius of curvature to width) is in the range between one and two. In the Cecina study site, the ratio is well within this range, although no chute cutoff yet has formed, as no large flood has occurred since the study bend matured. Though the Cecina River has many geomorphological similarities to the Welsh rivers studied by Lewis and Lewin (1983), the adjustment of bend geometry alone is not enough to account for the development of a chute cutoff and other factors, such as a sediment imbalance and the above mentioned dual set of formative discharge, need to be considered.

7. Discussion and conclusions

Channel pattern is controlled by the mutual interaction of many factors of which dominant discharge, often taken as $Q_{1.5}$ or $Q_{2.33}$, is regarded as sufficient to describe the hydrological part. In the case of Cecina River, however, it seems necessary to consider the effects of two different formative discharges to understand its pseudomeandering planform. Frequent, moderate floods are capable of shaping the river towards a meandering pattern, but this development is interrupted by large floods (Q_{10}–Q_{20}), which cut through the incipient point bars and force the main channel back towards a straight planform. A plot of channel gradient versus discharge (Leopold and Wolman, 1957) places the Cecina River in the braided category (though very close to the line that discriminates braided from meandering rivers), whereas, a plot of slope versus a combination of discharge and grain size (Parker, 1979), using the mean grain size of deposited material (2.9 mm), places the river just below the braiding threshold with $Q_{1.5}$ and very close to braiding with Q_{20}. As bank resistance plays a major role for the planform development, this factor should not be neglected. Ferguson (1973) suggested consideration of the bank content of fine grained material, but in the case of the study site, this is not possible since the cut bank consists mainly of coarse gravel (slightly cemented at the base) overlain by laminated sand and massive silt and clay. Use of the slope/Froude number ratio (S/Fr) in combination with depth/width ratio (d/w), as suggested by Parker (1976), seems to be an appropriate alternative since depth/width ratio is implicitly related to bank resistance. Both $Q_{1.5}$ and Q_{20} plot in the meandering part of Parker's (1976) diagram with Q_{20} close to the transition towards a straight channel pattern.

It is suggested here that the Cecina River's pseudomeandering morphology results from the combination of the following main factors.

(1) *Incision*—the present overbank (inner bar top) deposits are approximately 2 m lower than the old (probably Middle Age, Benvenuti, personal communication) flood plain. This in itself is not a distinctive factor for the development of pseudomeandering rivers, but nor are the resulting implications that follow.

(2) *Cohesive bank deposits*—the channel is prevented from braiding because of raised bank resistance: banks consists mainly of coarse gravel (in places slightly cemented at the base) overlain by a massive bench of fine grained, overbank deposits.

(3) *Sediment supply*—though in the study reach, the balance between incoming and outcoming sediment is negative, the sediment supply is sufficient for side bars to grow and deflect the flow towards the opposite banks during moderate floods. Therefore, bar growth is no longer the cause but merely the result of a vain attempt to fill up the space left by the rapidly retreating bank.

(4) *Flow regime*—During frequent, moderate floods, the morphology of the embryonic bends develops towards a meandering pattern through a gradual decrease of the radius of curvature. Infrequent, large floods (Q_{20}), being confined within an incised channel, have gradient and power enough to cut through the lateral bars and leave the incipient meander bends as inactive, lunate embayments in the elevated cut bank.

(5) *Flash floods*—the short duration of even large floods, in combination with the enhanced bank resist-

ance, prevents the river from channel-width-adjustments towards equilibrium during the largest floods.

On the existing basis, it is not possible to determine whether pseodomeandering channel morphology is a previously unrecognised type of stable river pattern or merely represents a transitional, unstable phase, following incision in the present setting. Nevertheless, the pseudomeandering river planform is very common in Tuscany, and so far the modern morphology of the Cecina River seems stable, in the long term, since it results from the balance of opposite tendencies to form meanders during frequent floods and to assume a straight course during infrequent, large floods. It could be argued that the development since 1954 (Figs. 4 and 5) represents the change from a straight towards a meandering planform in the new lower level of the incised river. Whether or not this development will be interrupted by the next very large flood forming a new straight planform remains to be seen. However, the Q_{20} simulations in the studied river reach, and the fact that the first formed bends were actually cut off by a flood between 1954 and 1986 (Fig. 4 at about 1000 m), speaks in favour of the suggested cyclic development.

Acknowledgements

This research benefited from funds provided by the two institutions involved. We are pleased to express our gratitude to Ditte, Mette and Anders for their assistance in the field, to Bjarne Fogh for his help with analysing the grain-size photos, to Kent Pørkesen for the layout assistance, Ulf Thomas and Paul Christiansen for the logistic, and to Kirsten Simonsen at the Skalling laboratory for the grain-size analysis. Gordon Grant reviewed an earlier version of the manuscript. We are pleased to express our gratitude for his good comments and linguistic corrections. Likewise, two anonymous referees are thanked for their valuable suggestions.

References

Ackers, P., Charlton, F.G., 1970. The geometry of small meandering streams. Proc. - Inst. Civ. Eng. S12, 289–317.

Allen, J.R.L., 1985. Principles of Physical Sedimentology. Allen & Unwin, London, 272 pp.

Ashley, G., 1990. Classification of large-scale subaqueous bedforms: a new look at an old problem. J. Sediment. Petrol. 60, 160–172.

Baker, V.R., Ritter, D.F., 1975. Competence of rivers to transport coarse bedload materials. Geol. Soc. Am. Bull. 86, 975–978.

Billi, P., Paris, E., 1992. Bed sediment characterisation in river engineering problems. In: Bogen, J., Walling, D.E., Day, T.J. (Eds.), Erosion and Sediment Transport Monitoring Programmes in River Basins, vol. 210. IAHS Press, Wallingford, pp. 11–20.

Billi, P., Rinaldi, M., 1997. Human impact on sediment yield and channel dynamics in the Arno River Basin (central Italy). IAHS Publ. 245, 301–311.

Billi, P., Losito, G., Muschietti, M., 1991. Geological setting, tectonic evolution and related seismic activity. In: Vannucchi, G. (Ed.), Seismic Hazard and Site Effects in the Florence Area. Dipartimento di Ingegneria Civile, Università di Firenze, Firenze, pp. 1–9.

Bridge, J.S., Smith, N.D., Trent, F., Gabel, S.L., Bernstein, P., 1986. Sedimentology and morphology of a low-sinuosity river: Calmus River, Nebraska Sand Hills. Sedimentology 33, 851–870.

Brocchi, L., 1987. Dinamica morfologica del Fiume Arno dalla confluenza con la Chiana alla Gonfolina. Caratteri morfologici. Unpublished M.Sc. Thesis, University of Florence, 92 pp.

Carmignani, L., Decandia, F.A., Disperati, L., Fantozzi, P.L., Lazzarotto, A., Liotta, D., Oggiano, G., 1995. Relationships between the Tertiary structural evolution of the Sardinia-Corsica-Provencal Domain and the Northern Apennines. Terra Nova 4, 128–137.

Carta Tecnica Regionale 1:5000, 1979. Regione Toscana.

Casagli, N., Rinaldi, M., Gargini, A., Curini, A., 1999. Pore water pressure and streambank stability: results from a monitoring site in the Sieve River, Italy. Earth Surf. Processes Landforms 24, 1095–1114.

Church, M., 1996. Channel morphology and typology. In: Petts, G., Carlow, P. (Eds.), River Flows and Channel Forms. Blackwell, Oxford, pp. 185–202.

Cognigni, G., 1996. Geomorfologia dell'alveo del Fiume Cecina. Unpublished M.Sc. thesis. University of Florence, 149 pp.

Dietrich, W.E., 1987. Mechanics of flow and sediment transport in river bends. In: Richards, K. (Ed.), River Channels. The Institute of British Geographars Special Publication 17, Blackwell, Oxford, pp. 179–227.

Engelund, F.A., Petersen, F.B., 1974. Hydraylik. Den private ingeniørfond, Danmarks Tekniske Højskole, 233 pp.

Ferguson, R.I., 1973. Channel pattern and sediment type. Area 5, 38–41.

Hickin, E.D., 1972. Pseudomeanders and point dunes—flume study. Am. J. Sci. 272, 762–799.

Ibbeken, H., Schleyer, R., 1991. Source and Sediment. A Case Study of Provenance and Mass Balance at an Active Plate Margin (Calabria Southern Italy). Springer, Berlin, 286 pp.

Jackson, R.G., 1975. Hierarchical attributes and a unifying model of bedforms composed of cohesionsless material and produced by shearing flow. Geol. Soc. Am. Bull. 86, 1523–1533.

Keller, E.A., 1972. Development of alluvial stream channels: a five-stage model. Geol. Soc. Am. Bull. 83, 1531–1536.

Komar, P.D., 1989. Flow-competence evolutions of the hydraulic parameters of floods: an assessment of the technique. In: Beven, K., Carling, P. (Eds.), Floods: Hydrological, Sedimentological and Geomorphological Implications. Wiley, Chichester, pp. 107–134.

Komar, P., 1996. Entrainment of sediments from deposits of mixed drain sizes and densities. In: Carling, P., Dawson, M.R. (Eds.), Advances in Fluvial Dynamics and Stratigraphy. Wiley, Chichester, pp. 127–181.

Laronne, J.B., Duncan, M.J., 1992. Bedload transport paths and gravel bar formation. In: Billi, P., Hey, R.D., Thorne, C.R., Tacconi, P. (Eds.), Dynamics of Gravel-Bed Rivers. Wiley, Chichester, pp. 177–202.

Lenzi, M., D'Agostino, V., Billi, P., 1999. Bedload transport in the instrumented catchment of the Rio Cordon: Part I. Analysis of bedload records, conditions and threshold of bedload entrainment. Catena 36, 171–190.

Leopold, L.B., Wolman, M.G., 1957. River channel patterns—braiding, meandering and straight. U.S. Geol. Surv. Prof. Pap. 282B, 39–85.

Lewin, J., 1976. Initiation of bed forms and meanders in coarse-grained sediment. Geol. Soc. Am. Bull. 87, 281–285.

Lewis, G.W., Lewin, J., 1983. Alluvial cutoffs in Wales and the borderlands. In: Collinson, J.D., Lewin, J. (Eds.), Modern and Ancient Fluvial Systems. IAHS Spec. Publ. 6. Blackwell, Oxford, pp. 145–154.

Parker, G., 1976. On the cause and characteristic scale of meandering and braiding in rivers. J. Fluid Mech. 76, 459–480.

Parker, G., 1979. Hydraulic geometry of active gravel rivers. J. Hydraul. Div., Am. Soc. Civ. Eng. 105, 1185–1201.

Rinaldi, M., Casagli, N., 1999. Stability of streambanks formed in partially saturated soil and effects of negative pore water pressures: the Sieve River (Italy). Geomorphology 26, 253–277.

Schumm, S.A., 1977. Fluvial System. Wiley, New York, 338 pp.

Smith, J.D., McLean, S.R., 1984. A model for flow in meandering streams. Water Resour. Res. 20, 1301–1315.

Teruggi, L.B., Billi, P., 1997. Sedimentology of a pseudomeandering river (Cecina R., central Italy). G. Geol. 59 (1–2), 267–272.

Williams, G.P., 1978. Bankfull discharge of rivers. Water Resource Research 14, 1141–1158.

Williams, G.P., 1983. Paleohydrological methods and some examples from Swedish fluvial environments. Geogr. Ann. 65A, 227–244.

Winchips, 1998 Published by the Institute of Geography, University of Copenhagen. http://www.lh@geogr.ku.dk.

Yalin, M.S., 1992. River Mechanics. Pergamon, Oxford, 220 pp.